

PCO₂, chemical properties, and estimated new production in the equatorial Pacific in January-March 1991

Nathalie Lefèvre, Chantal Andrié, and Yves Dandonneau

Laboratoire d'Océanographie Dynamique et de Climatologie, University of Paris VI/ORSTOM/CNRS

Gilles Reverdin¹

Lamont-Doherty Earth Observatory, Palisades, New York

Martine Rodier

Institut Français de Recherche Scientifique pour le Développement en Coopération (ORSTOM), Nouméa, New Caledonia

Abstract. Measurements of the partial pressure of CO₂ (PCO₂) at the sea surface, dichlorodifluoromethane (F12), salinity, temperature, oxygen, nutrients, wind, and current velocities were made during a cruise (January-March 1991) in the equatorial Pacific from Panama to Nouméa via Tahiti. In the western Pacific (140°W to 165°E) the westward South Equatorial Current is well established. Distributions of tracers show extrema near the equator in the eastern Pacific (from 95°W to 140°W), indicating that the upwelling is especially active in this area. The zonal distribution of chemical tracers is not regular because of intrusions of warmer water from the north associated with equatorial long waves. The temporal changes in PCO₂ result from thermodynamic changes, biological activity, and gas exchange with the atmosphere. In order to compare the magnitude of these processes, we assess the variations of PCO₂ (dPCO₂) between two stations as the sum of thermodynamic changes driven by temperature and salinity changes, air-sea exchange computed from observed wind and difference of PCO₂ between the sea and the atmosphere, and the biological activity estimated from the nitrate decrease and C:N ratio (106:16). The resulting assessed change in PCO₂ is in agreement with the observed change for 42 pairs of stations. Each of these pairs of stations is thus considered as representing a simple water mass advected by the measured currents between the two stations so that daily fluxes can be estimated. The contribution of CO₂ outgassing to dPCO₂ is low, between -0.2 to -0.0 μatm d⁻¹. The thermodynamical dPCO₂ averages 0.7 ± 0.2 μatm d⁻¹ in the mixed layer. The biological dPCO₂ (-1.5 ± 0.5 μatm d⁻¹) is the highest in absolute value implying an average value of new production along the equator of 72 ± 25 mmolC m⁻² d⁻¹ (0.9 ± 0.3 gC m⁻² d⁻¹) for the equatorial Pacific (130°W-165°E). This value is very high and the overestimation could result from the simplistic description of the advection and mixing of water. An attempt to account for these processes by constraining the net heat flux to 100 W m⁻² [Weare *et al.*, 1981] reduces the estimate of new production to 58 mmolC m⁻² d⁻¹ (0.7 gC m⁻² d⁻¹). A mean upwelling velocity of 0.5 ± 0.1 m d⁻¹ east of 140°W is calculated, based on F12 undersaturations.

Introduction

The evolution of various advected properties of a body of water can be quantified by estimating the fluxes into the water. In certain areas, where horizontal advection is negligible, data collected at time series stations are well adapted for such purposes. Thomas *et al.* [1990], Wong and Chan [1991], and Garçon *et al.* [1992] have thus assessed the role of photosyn-

thesis in the annual cycle of carbon dioxide and oxygen at station P in the North Pacific. In other areas, surface water drifts are important and measuring concentrations at a fixed point is not sufficient for estimating fluxes. The diurnal variations in surface partial pressure of carbon dioxide (PCO₂) and O₂ have been assessed along a drogue track during the North Atlantic Bloom Experiment [Robertson *et al.*, 1993]. The changes in O₂ and PCO₂ were used to estimate net community production and photosynthetic quotients.

Assessing the biogeochemical fluxes in the equatorial Pacific is of major importance for the Joint Global Ocean Fluxes Studies (JGOFS) objectives because the equatorial upwelling is a strong source of CO₂ for the atmosphere [Broecker *et al.*, 1986; Feely *et al.*, 1987; Murphy *et al.*, 1991; Inoue and Sugimura, 1992; Lefèvre and Dandonneau, 1992; Wong *et al.*, 1993]. Warming of upwelled waters with high-carbon content and an intense biological activity [Chavez and Barber, 1987;

¹ Also at Laboratoire d'Océanographie Dynamique et de Climatologie, University of Paris VI/ORSTOM/CNRS.

Copyright 1994 by the American Geophysical Union.

Paper number 94JC00293.
0148-0227/94/94JC-00293\$05.00



—

Dugdale *et al.*, 1992] are the main processes responsible for the CO₂ variations. This was the prime motivation for the experiments carried out in 1992 along 140°W for the JGOFS program.

In the present work we use the results of 111 stations made during the cruise (January-March, 1991) in the equatorial Pacific from 95°W to 165°E. The first section discusses sampling and analytical methods. The distribution of surface properties along the equator and on meridional transects is presented in the second section. Property distributions (presented in detail in the appendix) are discussed in the third section using parameter-parameter plots (PCO₂, nitrate, sea surface temperature (SST), and F12) in order to distinguish the relative effects of the surface warming, the upwelling, and the biological consumption on the PCO₂ distributions. In the fourth section we separate physical and biogeochemical factors which influence the PCO₂ (i.e. nitrate, temperature variations and CO₂ evasion to the atmosphere) to simulate PCO₂ variations. New production is estimated when the PCO₂ given by this simulation matches the measured PCO₂. In the eastern Pacific an estimate of the upwelling velocity and new production are done using F12 undersaturations.

The track followed during the cruise ALIZE 2 was mainly along the equator with five short meridional sections (95°W, 110°W, 125°W, 168°W and 165°E) and a section along 140°W followed by a port of call in Tahiti where the ship stopped for 3 days and then sailed northward along 149°W. Figure 1 shows the route of the ship and the direction of the observed surface current. Hydrological and current data are presented by Reverdin *et al.* [1991] and Eldin *et al.* [1992]. During the cruise the trade winds blew from the south-east near the equator from 110°W to 180°W and they were slightly stronger than the climatological monthly winds [NOAA, 1991]. Meridional winds also seem to have been stronger but they show weaker variations than the zonal component. From 180°W to 165°E average winds were weak but highly variable.

During the cruise, the sea surface temperature was lower at the equator than at 2.5°S or 2.5°N from 95°W to 140°W (see the appendix) suggesting that the equatorial upwelling is still present. SST distributions compared with those obtained in November and December 1990 [NOAA, 1990] suggest that the upwelling was weakening. The temperatures were also about 2°C higher than those found by other authors [Feely *et al.*, 1987; Inoue and Sugimura, 1992; Wong *et al.*, 1993] reinforcing this hypothesis. The equatorial divergence appears very clearly on drifting buoy trajectories, especially in the eastern Pacific [NOAA, 1991]. Along the equator the sea surface temperature increases from east to west (23°C to 30°C; see

the appendix). In the eastern Pacific from 95°W to 127°W, fluctuations in the temperature front associated with large meridional current fluctuations were present. West of 127°W the westward zonal current is well established and the meridional current fluctuations are weaker.

Sampling and Analytical Methods

Continuous measurements of currents and PCO₂ were made along the route followed by the ship. Conductivity temperature depth (CTD) casts to 1000 or 2000 dbar were obtained every 2° on the equator and every 0.5 degree on the meridional sections using a Neil-Brown Mark III probe fitted with a 12-bottle rosette sampler. Samples were taken in the upper ocean at 111 CTD casts for measurements of oxygen, nutrient (nitrate, phosphate, and silicate), chlorophyll *a*, and dichlorodifluoromethane (CCl₂F₂ or F12, only for stations 7 to 69). Eleven samples were taken at each cast in the layer from 0 to 500 m depth. Using 12 samples at each station, CTD salinity was calibrated with a Portasal salinometer from Guildline (accuracy better than 0.01). CTD temperature was calibrated before and after the cruise (drift less than 0.01°C).

Current measurements were made with a 150 kHz acoustic doppler current profiler (ADCP) from RD Instruments. The ADCP transducer was placed in a well 4 m below sea surface. The depth range of the ADCP varied from 250 to 270 m. Zonal and meridional velocities are obtained with an error of ±5 cm s⁻¹ on individual measurements. GPS navigation was used to compute absolute velocities [Eldin *et al.*, 1992].

PCO₂ was measured using an open circuit equilibrator and a Siemens® infra-red CO₂ analyzer calibrated twice a day. Sea water was taken at 2 m depth and pumped to an air-sea equilibrator with an open air circuit. Air-sea CO₂ equilibrium is achieved in the main pipe of a "water pump" (i.e., a T tube commonly used to suck in air through the pipe at right angles when water flows through the main pipe, but which is used here to initiate an air loop to and from the equilibrator at atmospheric pressure). Air bubbles and water are separated in a plexiglass® box from which water escapes through a siphon [Lefèvre and Dandonneau, 1992]. Because of the high flow rate of water, the temperature variations in the water circuit were less than 0.1°C, measured with thermistors placed in the equilibrator and at the water intake. The system was alternately operated on atmospheric air and on equilibrated air with commutation occurring once every 10 min. One value of PCO₂ in sea water and one value of pCO₂ in the atmosphere were recorded during each 20-min cycle. The mole fraction xCO₂ in dry air was converted into partial pressure using

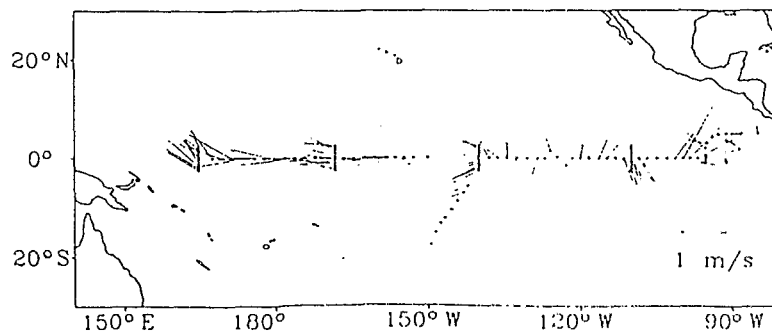


Figure 1. Cruise track with surface current direction.

$$PCO_2 = xCO_2(P_{atm} - p_{H_2O}) \quad (1)$$

where $P_{atm} = P/1023.15$ is obtained from a pressure sensor placed inside the main compartment of the equilibrator (P in hPa) and p_{H_2O} is computed at the interface conditions for the temperature variation in the water circuit using the formula given by *Oudot and Andrié* [1989]. For the small range of temperature variations ($dT < 0.1^\circ\text{C}$) this formula gives similar results to those presented by *Copin-Montégut* [1988, 1989]. The instrumental error on PCO_2 (nonconstant drift of the CO_2 analyser between two consecutive calibrations) could not be separated from the small-scale variability during the cruise ALIZE 2. The average variability over distances less than 30 km was 8 μatm (one standard deviation).

Nutrients were analyzed from station 9 to station 113, following the method of *Strickland and Parsons* [1972] with a Technicon Autoanalyzer II, GF/F. For nitrate concentrations less than 2 $\mu\text{mol l}^{-1}$ the high-sensitivity method described by *Oudot and Montel* [1988] was used.

Dichlorofluoromethane (F12) samples have been taken with 100 ml syringes from each Niskin bottle of station 7 to station 69. Unfortunately, the trichlorofluoromethane (F11) data had to be rejected because of a contamination of the bottles. The F11 contamination ranges between 5 to 20 times the oceanic surface concentration, depending on the sampling bottles. The estimated F12 contamination varies depending on the F11 contamination level but is always less than a few percent of the total F12 signal. A minor F12 correction related to the contamination has been accounted for. The samples were analyzed by a chromatographic method [*Bullister and Weiss*, 1988] with electron capture detection and data are reported on the Scripps Institution of Oceanography (SIO) scale. The detection limit was around 0.05 pmol kg^{-1} with a reproducibility on surface samples on the order of 1%. Data are expressed in percentage deviation from atmospheric solubility equilibrium [*Warner and Weiss*, 1985].

Seawater samples of 100 ml were collected and filtered on Whatman GFF filters for chlorophyll *a* estimation. The filters were frozen and analyzed at the ORSTOM laboratory in Nouméa (New Caledonia) using the instructions outlined by *Le Bouteiller et al.* [1992].

Surface Hydrological and Chemical Properties

Figure 2 shows the zonal spatial structure of surface properties during the cruise. The upwelling is active especially in the eastern Pacific. The highest surface values of nutrients are observed around 95°W , associated with F12 undersaturations with respect to the atmosphere, and are located near the equator. Maxima in PCO_2 and nutrients observed south of the equator (2.5°S) at 110°W suggest that upwelled water has been drifting at the surface for a few days. A detailed description of the property distributions is given in the appendix.

The distributions of chemical properties were disturbed by the intrusion of warmer and less dense waters due to equatorial long waves both at the equator at 128°W and north of the equator along the 110°W transect. The waters were nutrient-depleted, undersaturated in CO_2 and near the F12 equilibrium conditions with the atmosphere.

From 140°W to 165°E , no cold upwelled water was observed at the surface. Nutrients values decrease westward while the

temperature increases. The PCO_2 values remain high which probably result from advection and warming. In the central Pacific a westward current was well established and the dominant process was the warming, together with biological activity.

The PCO_2 evolution is controlled by biogeochemical and physical processes. In order to separate the different processes responsible for the PCO_2 distribution, we have studied PCO_2 (or F12) versus temperature plots and PCO_2 versus NO_3 plots.

We observe large differences along the equatorial section. Because the upwelling decreases to the west the water becomes poorer in nutrients and gaseous CO_2 as it is warmed. The PCO_2 -SST plot (Figure 3a) clearly distinguishes the upwelling input (high PCO_2 and low temperature) in the 95°W area from waters warmed further at 140°W - 149°W . The upwelling effect is shown on the F12-temperature plot (Figure 3e). The plot of F12 undersaturations versus the temperature is also given for the 95°W data at 30 m depth. The regression line (slope = 9.87; correlation coefficient $r = 0.97$) is given as an empirical reference for the upwelling influence. The surface data at 95°W lie near the regression line and show important undersaturations (down to -10%). Station 8 (2.07°N , 95.40°W) is subject to a warm water flow (SST = 25.8°C) associated with F12 near saturation (-1.1%) and presents a PCO_2 (328 μatm) below the atmospheric PCO_2 value (349 ± 5 μatm).

At 110°W , the north-south gradient shown on the meridional distribution (see the appendix) appears clearly on Figure 3a. The effect of the upwelling is persistent only to the south. The temperature and the salinity of the water in the northern part of the transect at 110°W were close to those of the water at 95°W , 2°N , indicating that they both originated from intrusions of warm oligotrophic water from the north caused by equatorial long waves [*Eldin et al.*, 1992].

On the 140°W - 149°W transect to Tahiti, the F12-SST plot (Figure 3e) does not show a significant trend and the upwelling effect does not appear. The PCO_2 -SST plot (Figure 3a) shows an unexpectedly high negative correlation ($r = -0.98$). The slope of the PCO_2 -SST plot has the opposite sign of that expected if warming of surface water was mainly responsible (the commonly admitted 4% increase per degree Celsius [*Copin-Montégut*, 1988]). It likely results from biological activity in addition to mixing with CO_2 equilibrated warm waters from the south tropical Pacific. Negative slope between PCO_2 and SST was also observed by *Watson et al.* [1991] in a phytoplanktonic bloom. They explained it as a result of biological activity rather than physical mechanism. Moreover, they observed a strong covariation of chlorophyll and carbon. We do not observe a strong correlation between PCO_2 and chlorophyll in the equatorial Pacific, where the grazing is often considered to play an important role [*Walsh*, 1976; *Cullen et al.*, 1992; *Minas and Minas*, 1992]. From 140°W to 165°E we observe a strong PCO_2 -SST negative correlation ($r = -0.91$, Figure 3b). The tendency to have a 24 μatm PCO_2 decrease per 1°C increase is again suggesting that the warming effect does not determine this spatial structure.

Hence the PCO_2 -SST relationship is always different from the 4% per degree Celsius temperature effect which contrasts with the PCO_2 -SST correlation observed in the equatorial Atlantic ocean [*Smethie et al.*, 1985, *Andrié et al.*, 1986]. It is interesting to note that this happens despite similar east-west temperature gradients in the two oceans. The importance of biological activity for the change of PCO_2 in the equatorial

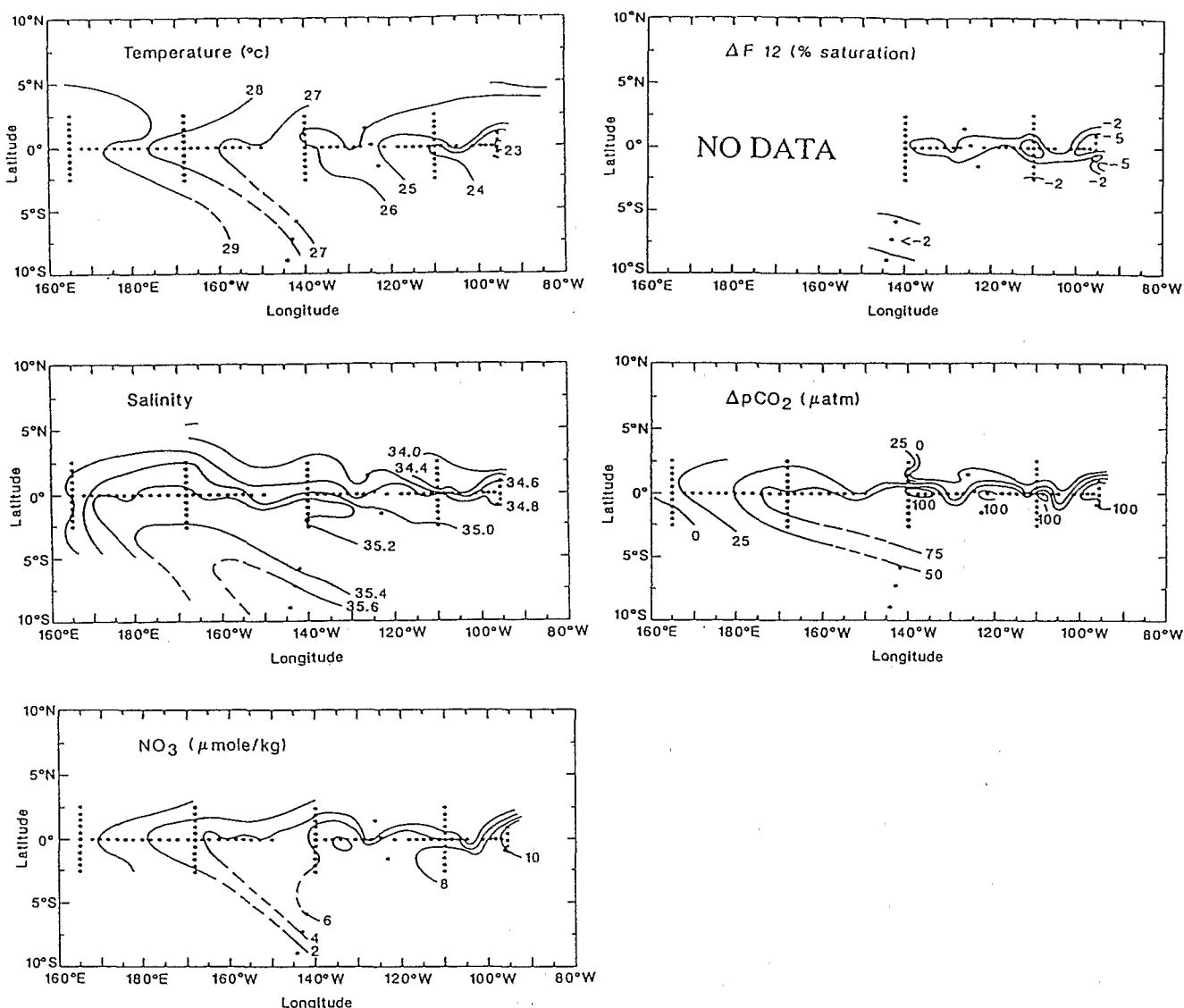


Figure 2. SST, F12, salinity, $\Delta p\text{CO}_2$, NO_3 , surface distributions. The dots represent station positions.

Pacific will be illustrated by discussing the relation of PCO_2 with other nutrients.

On the PCO_2 - NO_3 plot (Figure 3c) the high PCO_2 and nutrient concentrations correspond to the colder waters, and the warmer station 20 (0° , 104.53°W) (SST = 25.4°C) is poor in nutrients ($\text{NO}_3 = 1.85 \mu\text{mol l}^{-1}$). We interpret the north-south difference at 110°W as an influence of upwelling to the south, and of the north equatorial countercurrent to the north.

At 140°W - 149°W the PCO_2 - NO_3 correlation is very strong ($r = 0.99$). As shown by the F12 meridional distribution the upwelling was less active at 140°W but we noticed that a southwestward current transports the water which was upwelled farther east. This water, initially rich in PCO_2 and nutrients, possibly mixes with oligotrophic nutrient-depleted waters equilibrated with the atmosphere; in addition nutrients are also depleted during advection. PCO_2 is well correlated with SST ($r = -0.98$) and NO_3 ($r = 0.93$) at 95°W but the correlation with SST is a little stronger, suggesting that this distribution of PCO_2 is related to water masses. We can assume that a weak consumption by phytoplankton decreases the stock of nitrates and of total CO_2 . The weak consumption has a relatively small effect on the CO_2 , which is never a limiting

factor for biological activity. The correlations with nitrate (PCO_2 - NO_3 , SST- NO_3) are then not so high as a correlation including only dynamic properties. From 140°W to 165°E we observe a positive correlation between PCO_2 and NO_3 ($r = 0.92$) (Figure 3d) and a negative correlation between PCO_2 and SST ($r = -0.91$) (Figure 3b). As westward surface currents were well established from 127°W to 165°E , we can assume that the upwelled water, rich in CO_2 and nutrients, flowed westward and that the biological activity and/or an upwelling of warmer water explain the decrease of both PCO_2 and nitrates. The zero level of nitrate observed at 165°E is likely the result of a consumption by phytoplankton and/or a mixing with oligotrophic waters.

Estimate of Upwelling Velocity in the Eastern Pacific

For the eastern Pacific, for which F12 was measured, we estimate an upwelling velocity, assuming that the surface equatorial water is upwelled water modified by exchange with the atmosphere only and that the system is stationary on the short time scale which corresponds to the equilibration time

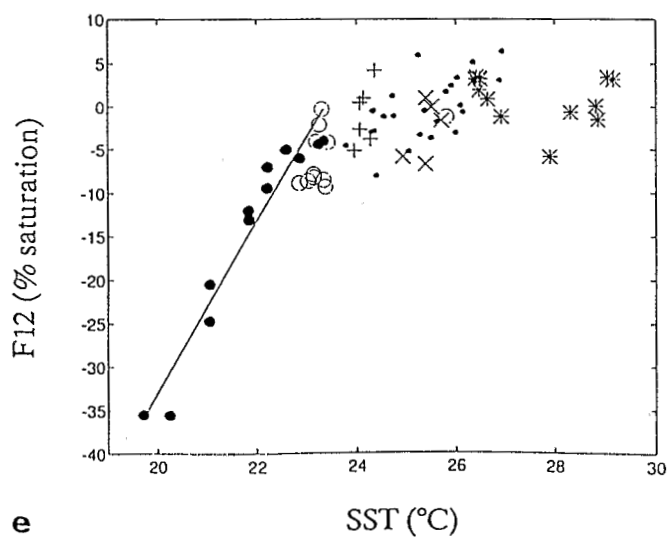
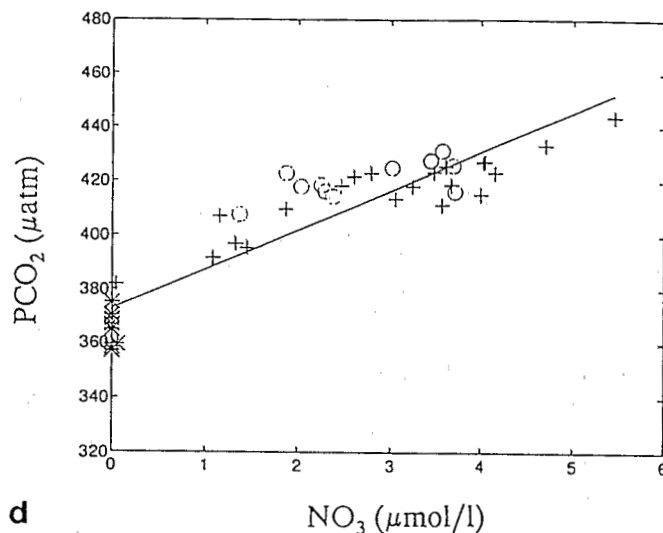
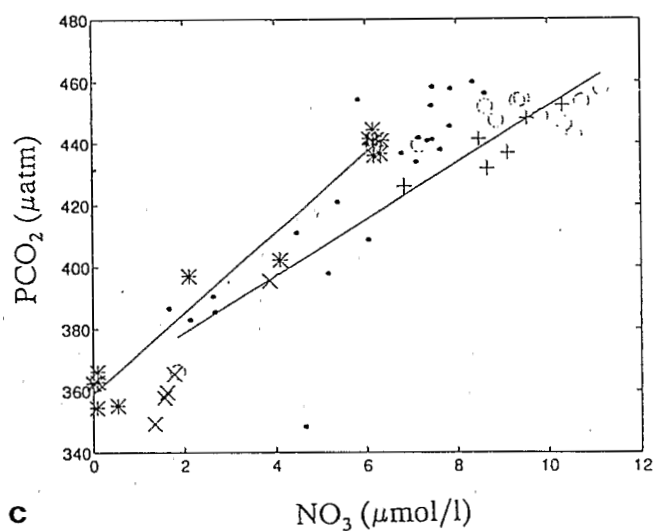
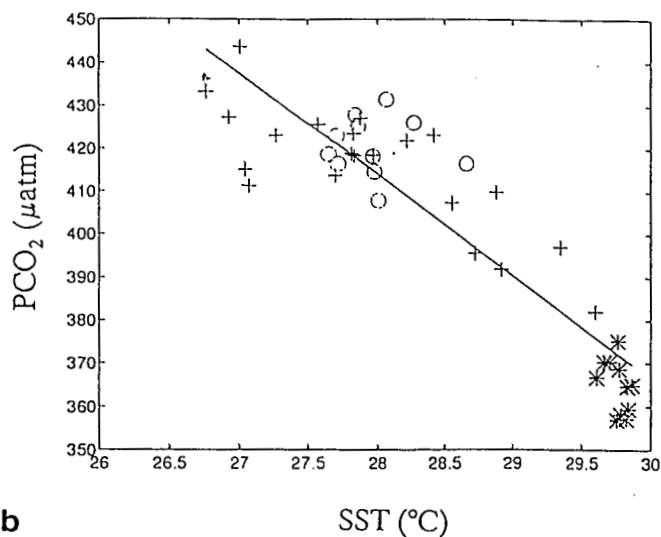
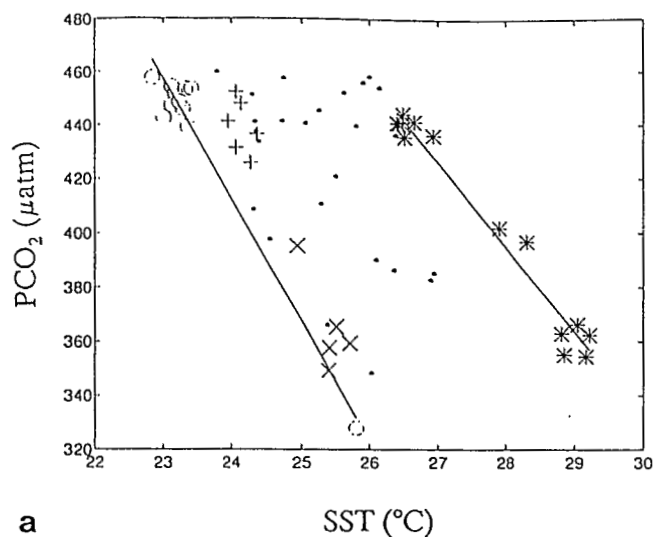


Figure 3. (a) PCO₂-SST scatter plot from 95°W to 140°W. Open circles represent data along 95°W, pluses represent data south of the equator along 110°W, crosses represent data north of the equator at 110°W, asterisks represent data along 140°W-149°W, and dots represent data at the equator. (b) PCO₂-SST scatter plot from 140°W to 165°E. Open circles represent data along 168°W, asterisks represent data along 165°E and pluses represent data elsewhere. (c) PCO₂-NO₃ scatter plots from 95°W to 140°W. Open circles represent data along 95°W, pluses represent data south of the equator along 110°W, crosses represent data north of the equator at 110°W, asterisks represent data along 140°W-149°W, and dots represent data at the equator. (d) PCO₂-NO₃ plots from 140°W to 165°E. Open circles represent data along 168°W, asterisks represent data along 165°E and pluses represent data elsewhere. (e) F12-SST scatter plot from 95°W to 140°W. Open circles for surface data along 95°W, dark circles for data at 30 m depth, pluses for data south of the equator along 110°W, crosses for data north of the equator along 110°W, stars for data along 140°W-149°W and dots for data at the equator.

of the surface layer with the atmosphere (on the order of 1 month). The depth from which the upwelled water originates (z) is considered to be between 40 and 100 m for the eastern Pacific [Fiedler *et al.*, 1992]. In this work we consider z about 10 m deeper than the depth where F12 concentration starts diminishing (z ranges between 50 and 110 m from 95°W to 140°W). The upwelled flux of F12 is $w \times (F12_0 - F12_z)$, where w is the upwelling velocity, $F12_0$ is the F12 concentration in surface waters, and $F12_z$ is the F12 concentration at the depth z . The flux of F12 exchanged at the air-sea interface is $k_{F12}(F12_{sat} - F12_0)$ where k_{F12} is the F12 transfer coefficient [Warner, 1988] and $F12_{sat}$ is the saturation value of F12. The upwelling velocity can then be obtained as

$$w = k_{F12} \times (F12_{sat} - F12_0) / (F12_0 - F12_z) \quad (2)$$

West of 130°W the mixed layer is deeper and the property distributions (see the appendix) do not show cold nutrient-rich upwelled water. Moreover, surface waters are supersaturated in F12. In some cases the distribution of F12 does not provide a positive velocity ($F12_{sat} < F12_0$ due to warmed surface waters): The upwelling velocity is then set equal to zero and is not taken into account in the average. The average upwelling velocity (calculated with 27 stations) for the eastern Pacific (95°W to 130°W) is estimated as $0.5 \pm 0.1 \text{ m d}^{-1}$ (extremes are 0.0 m d^{-1} and 1.3 m d^{-1}). Feely *et al.* [1987] interpreted apparent F12 undersaturations in the same way to yield mean upwelling velocity on the order of $0.1\text{--}1 \text{ m d}^{-1}$. Wyrki [1981] estimates a resulting vertical upwelling at 1 m d^{-1} but assumes that the actual upwelling velocity at the equator could be much larger. Halpern [1980] found a maximum velocity at 2.5 m d^{-1} at the equator near 110°W. More recently, Halpern *et al.* [1989] estimated a 2 m d^{-1} upwelling velocity. The average value of 0.5 m d^{-1} obtained here is low, which suggests that the upwelling was weak during the cruise. This is supported by the study of the seasonal climatology of currents by Poulain [1993], which shows that the upwelling velocity is weaker during the northern winter. The SST distributions compared with the distributions a few months earlier [NOAA, 1991] and comparison with other studies [Feely *et al.*, 1987; Wong *et al.*, 1993] confirm this hypothesis (see the description at 168°W, for example, in the appendix).

Estimates of PCO₂ Changes and New Production

As we have seen in a previous section (Surface Hydrological and Chemical Properties), the distribution of PCO₂ cannot be explained by one single process. Here we estimate physical, chemical, and biological processes affecting the distribution of PCO₂ by modeling the observed variation of PCO₂ between two stations. The method that we use is based on the assumption that the water masses advect horizontally between pairs of stations: i.e., we do not take into account horizontal or vertical mixing nor equatorial upwelling. The observed currents at the time of the cruise define these advection paths, and a model of the PCO₂ changes is used to test which of these paths are compatible with the above assumptions. In the eastern Pacific the upwelling velocity estimated by F12 measurements is low and the upwelling effect will be discussed later. In addition to the limits relative to the dynamics, this

treatment is approximative because we did not measure the TCO₂ concentration and buffer factor.

We examine all station pairs, A (upstream) and B (downstream) consecutive or not, but not separated by more than 1000 km, and retain those for which we can admit that station B water results from a drift of station A water.

Principles of Carbon Flux Estimates

PCO₂ changes ($d\text{PCO}_2$) are caused by thermodynamics (SST and salinity), biological activity, and CO₂ evasion:

(a) Thermodynamic changes ($d\text{PCO}_2(T, S)$) are computed for SST according to Oudot and Andrié [1989]:

$$\ln \text{PCO}_2 = \ln \text{PCO}_{2u} + (T - T_u) \cdot (4.17 \times 10^{-2} - 3.78 \times 10^{-6} \text{PCO}_{2u}) \quad (3)$$

where T_u and PCO_{2u} are the upstream observations. This formula gives results that are very close to those obtained using Copin-Montégut's [1988, 1989] relationship.

(b) The salinity dependence of PCO₂ is expressed by the Weiss *et al.*'s [1982] relationship:

$$d(\ln \text{PCO}_2)/dS = 0.08620 - 1.272 \cdot 10^{-3} S_u \quad (4)$$

(c) The biological activity, reflected in changes of the surface water nutrient concentrations, leads to a PCO₂ change ($d\text{PCO}_2(\text{bio})$) using the Redfield ratio 106:16 and assuming a buffer factor of 8.5 (Inoue and Sugimura, 1992):

$$d\text{PCO}_2(\text{bio}) = ((106/16)d\text{NO}_3 / \text{TCO}_2) \times 8.5 \text{PCO}_2 \quad (5)$$

Dugdale *et al.* [1992] measured C:N uptake ratios with ¹⁴C and ¹⁵N, respectively, along a meridional section at 150°W in the equatorial Pacific. Their value at the equator (7.37) is close to the Redfield value.

(d) The CO₂ exchange with the atmosphere (F) was previously estimated [Lefèvre and Dandonneau, 1992] using the Liss and Merlivat's [1986] relationship, shipboard winds, and PCO₂ measurements during the cruise ALIZE 2. The variation of PCO₂ due to the flux ($d\text{PCO}_2(\text{atm})$) is calculated by:

$$d\text{PCO}_2(\text{atm}) = -8.5 \text{PCO}_{2u} \times F / (\text{TCO}_{2u} \times H \times v) \quad (6)$$

where TCO_{2u} is the upstream concentration of total inorganic carbon. We adopted a constant TCO₂ value equal to $2040 \mu\text{mol kg}^{-1}$ as done by Inoue and Sugimura [1992]. Specifying other TCO₂ values in the realistic range from 2000 to $2050 \mu\text{mol kg}^{-1}$ leads to a variation of $d\text{PCO}_2(\text{bio})$ and $d\text{PCO}_2(\text{atm})$ less than only $1 \mu\text{atm}$, which is negligible compared to the range of variations investigated. H is the depth of the mixed layer, F is the CO₂ flux, l is the distance between two stations, and v is the current velocity. The flux and the current velocity are averaged between the upstream and the downstream stations. The depth of the mixed layer is estimated from the temperature and density profiles at each station [Reverdin *et al.*, 1991] and ranges between 20 and 125 m.

Results of this computation give a value of downstream PCO₂ which is then compared with the observed PCO₂ value. We rejected A-B pairs for which the difference between predicted and observed PCO₂ was greater than the short-term variations of PCO₂ (i.e., greater than $8 \mu\text{atm}$, which corresponds to the

average standard deviation of the PCO₂ observations over less than 30 km.

For a valid assumption of water advection the current must flow from the upstream station A in the direction of the downstream station B. We assign that the observed current vectors must not diverge from the A to B direction by more than 45°.

Results and Discussion

Table 1 shows all pairs of stations which satisfied the conditions listed above and the corresponding dPCO₂. The dPCO₂ values are divided by the drift time l/v between the two stations to convert them into daily dPCO₂. For each upstream station, there is often more than one downstream station. All the estimates of dPCO₂ for the corresponding pairs are

averaged prior to computing the overall average. Generally, dPCO₂(bio) is larger than dPCO₂(T, S) and even more than dPCO₂(atm) (Figure 4). The mean value of all the dPCO₂(bio) is $-1.5 \pm 0.5 \mu\text{atm d}^{-1}$, while the contribution of CO₂ outgassing is very small in all cases with an average value of $-0.1 \mu\text{atm d}^{-1}$, and the thermodynamical effect averages $0.7 \pm 0.2 \mu\text{atm d}^{-1}$ which reflects the east-west warming. The dispersion in biological fluxes is large (Figure 4) with a rms of 2.1 compared to a rms of 0.8 for thermodynamical fluxes.

It is noteworthy that the model did not work in the eastern Pacific, except for two station pairs. We attribute that to the nonzonal surface circulation between 95°W and 140°W (Figure 1), so that we are less certain of advection paths, and also to the unreasonable nature of the assumptions on stationarity

Table 1. Results of the Simulation for Each Pair of Upstream and Downstream Stations.

Longitude Upstream	Longitude Downstream	dNO ₃ μmol/l	dPCO ₂ μatm	dPCO ₂ (T,S) μatm	dPCO ₂ (bio) μatm	dPCO ₂ (atm) μatm	NP mmol m ⁻² d ⁻¹
137.92°W	140.00°W	-4.64	-53.6	2.6	-55.9	-1.4	237.9
137.92°W	140.00°W	-4.09	-51.1	4.1	-49.3	-1.6	209.7
150.00°W	152.85°W	-0.59	-11.8	-3.4	-6.9	-0.2	48.0
150.00°W	154.73°W	-0.16	-8.0	-4.2	-1.9	-0.2	9.7
150.00°W	160.55°W	1.30	20.6	0.0	15.2	-1.1	-33.0
152.85°W	154.73°W	0.43	3.8	-0.8	4.9	-0.2	-69.5
152.85°W	160.55°W	1.89	32.4	3.4	21.5	-1.1	-70.6
152.85°W	162.47°W	0.04	14.2	11.7	0.5	-0.9	-1.0
154.73°W	160.55°W	1.46	28.6	4.2	16.7	-1.0	-46.8
154.73°W	162.47°W	-0.39	10.4	12.6	-4.5	-0.7	8.2
154.73°W	164.62°W	-0.95	-1.6	14.7	-10.9	-1.6	16.0
156.42°W	158.32°W	-0.65	-6.0	2.3	-7.8	-0.6	77.1
160.55°W	162.47°W	-1.85	-18.2	9.0	-22.7	-0.2	268.0
162.47°W	164.62°W	-0.56	-12.0	2.1	-6.6	-0.4	34.9
162.47°W	168.25°W	-0.04	5.9	11.4	-0.5	-0.4	1.1
164.62°W	166.58°W	0.98	13.4	4.2	11.2	-0.1	-162.3
164.62°W	168.25°W	0.64	12.4	12.8	7.3	-0.2	-54.5
164.62°W	168.25°W	0.52	17.9	9.0	5.9	-0.2	-44.6
164.62°W	168.26°W	0.39	14.3	4.8	4.5	-0.3	-37.5
166.58°W	168.25°W	-0.34	-1.0	8.8	-4.0	-0.0	73.4
166.58°W	168.25°W	-0.46	4.5	5.0	-5.4	-0.0	100.0
166.58°W	168.26°W	-0.59	0.9	0.7	-7.0	-0.0	141.1
172.20°W	174.27°W	0.24	5.2	0.7	2.8	-1.0	-23.9
172.20°W	176.25°W	-0.78	0.1	2.3	-9.0	-1.2	-11.2
172.20°W	178.25°W	-0.46	4.8	10.4	-5.3	-1.4	16.7
172.20°W	179.75°E	-0.65	3.5	6.1	-7.5	-1.9	17.7
172.20°W	177.75°E	-2.09	-11.0	11.0	-24.1	-2.9	44.5
174.27°W	176.25°W	-1.02	-5.1	1.6	-11.9	-0.5	149.3
174.27°W	178.25°W	-0.70	-0.4	9.8	-8.2	-0.8	52.7
174.27°W	179.75°E	-0.89	-1.7	5.5	-10.4	-1.2	44.3
174.27°W	177.75°E	-2.33	-16.2	10.3	-27.2	-1.9	84.6
176.25°W	178.25°W	0.32	4.7	8.1	3.7	-0.1	-49.8
176.25°W	179.75°E	0.13	3.4	3.8	1.5	-0.3	-10.0
176.25°W	177.75°E	-1.31	-11.1	8.6	-15.1	-0.7	65.8
178.25°W	179.75°E	-0.19	-1.3	-4.3	-2.2	-0.1	40.4
178.25°W	177.75°E	-1.63	-15.8	0.5	-19.0	-0.2	169.0
179.75°E	177.75°E	-1.44	-14.5	4.8	-16.8	-0.1	296.7
175.75°E	173.82°E	-0.36	-3.7	2.6	-3.9	-0.1	60.9
175.75°E	169.75°E	0.43	14.2	4.5	4.7	-0.8	-19.0
173.82°E	171.75°E	0.24	5.2	9.4	2.6	-0.0	41.0
173.82°E	169.75°E	0.79	17.9	1.9	8.5	-0.2	64.5
171.75°E	167.75°E	-1.28	-14.9	0.4	-14.0	-0.1	115.7

NP is the new production. Variations in nitrates and dPCO₂ represent the difference between the value at the downstream station and the one at the upstream station.

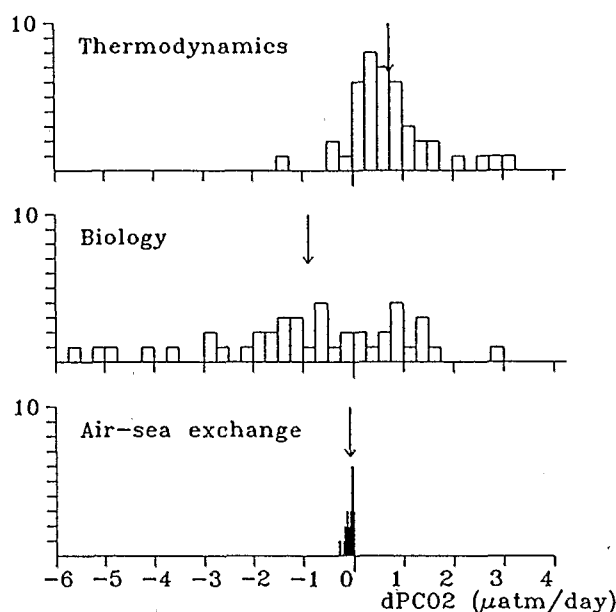


Figure 4. Histograms of thermodynamical $d\text{PCO}_2$, biological $d\text{PCO}_2$, and CO_2 outgassing from the simulation run between 95°W and 165°E (no pairs were included for the longitudes 95°W - 130°W because the condition $d\text{PCO}_2 < 8 \mu\text{atm}$ was never fulfilled). The ordinate axis represents the number of estimates for each $0.25 \mu\text{atm d}^{-1}$ bar for $d\text{PCO}_2(\text{T.S})$ and $d\text{PCO}_2(\text{bio})$ and for each $0.05 \mu\text{atm d}^{-1}$ bar for $d\text{PCO}_2(\text{atm})$. The arrows represent the average value for each term.

and to the neglect of horizontal and vertical mixing and vertical upwelling. All these terms are expected to contribute in the eastern Pacific, where we have found traces of equatorial long waves [Eldin *et al.*, 1992] and of upwelled water in the surface layer.

We did not find evidence for an east-west gradient in the thermodynamical and biological fluxes. Indeed for this cruise, *Le Bouteiller and Blanchot* [1991] show an homogeneity in the zonal distribution of phytoplankton for the whole enrichment area due to equatorial upwelling.

For the plausible upstream and downstream stations, daily rates of new production (NP) can be estimated as follows :

$$NP = \frac{d\text{NO}_3}{dt} \times H \times v \quad (7)$$

They are presented in Table 1. The average value of NP is estimated at $0.9 \pm 0.3 \text{ gC m}^{-2} \text{ d}^{-1}$. This value is high compared with other estimates: *Chavez and Barber* [1987] estimate a new production for 90°W - 180°W , 5°S - 5°N , of $1.9 \cdot 10^{15} \text{ gC yr}^{-1}$ ($0.40 \text{ gC m}^{-2} \text{ d}^{-1}$) using *Wyrki's* [1981] model. *Wong et al.* [1993] estimate that NP was reduced by 0.180 - $0.360 \text{ gC m}^{-2} \text{ d}^{-1}$ during the 1986-1987 El Niño event. *Dugdale et al.* [1992] found a NP of only $0.113 \text{ gC m}^{-2} \text{ d}^{-1}$ for equatorial stations at 150°W . Our estimate of NP is unprecise and probably too large.

The somewhat unrealistic hypothesis that water from station A could flow to station B can be tested against a similar approach involving the estimation of the net heat flux into the mixed layer. The average heat flux in the mixed layer for the selected pairs of stations is 180 W m^{-2} , and this value is higher than the global mean value of 100 W m^{-2} given by

Weare et al. [1981]. The excess of 80 W m^{-2} can be the result of mixing with neighbouring warmer waters. This difference leads to a $0.016^\circ\text{C d}^{-1}$ increase which can be converted in a reduction of the NP by $0.2 \text{ gC m}^{-2} \text{ d}^{-1}$ using the Redfield ratio and assuming that the NO_3 -T slope at the surface is equal to $2 \mu\text{M}$ per degree Celsius (as indicated by the measurements at 140°W and by unpublished results from the centre ORSTOM de Nouméa, 1988). However the heat flux is a poor constraint as our high value can be the result of high spatial and temporal variabilities in the current and thermal fields rather than of pure mixing.

In this computation the upwelling was not taken into account. The simulation using the previous estimates of upwelling velocity did not change the selection of pairs of stations in the eastern Pacific (very few pairs of stations verified the conditions for advection in the east because of the variable surface currents). A weak upwelling velocity has a small effect on our estimates of the CO_2 changes. We should, however, comment that the upwelling velocity provides an independent way to estimate "local" NP by considering the local supply of nitrate in the mixed layer using the relationship :

$$NP = w \times (106/16) \times (\text{NO}_{3z} - \text{NO}_{30}) \quad (8)$$

where NO_{3z} is the nitrate concentration at the depth z and NO_{30} is the value in surface waters. Despite the large uncertainty in vertical velocity due to the choice of depth for the upwelled water, the uncertainty is less for NP because the same level is retained for F12 and NO_3 . This estimate of NP where upwelling occurs averages only $11.4 \pm 1.8 \text{ mmolC m}^{-2} \text{ d}^{-1}$ ($0.14 \pm 0.02 \text{ gC m}^{-2} \text{ d}^{-1}$, extremes are 0.3 and $38 \text{ mmolC m}^{-2} \text{ d}^{-1}$) from 95°W to 130°W . The NP due to local upwelling should be smaller in the western Pacific where no large nitrate supply from deep waters is found (see the appendix).

Conclusions

The ALIZE 2 cruise was an attempt to collect dynamical, CO_2 , and tracer data in a quasi-synoptic fashion across the equatorial Pacific and provides an interesting data set for early 1991. We will mention the limitations of this survey: in particular the absence of CFC measurements in the western Pacific which would have allowed estimations of upwelling velocities and the lack of reliable primary production measurements. Also the synoptic circulation pattern is only partially known and the presence of long waves in the eastern Pacific is responsible for the difficulty in interpreting the PCO_2 data in the eastern Pacific.

The surface property distributions show that the upwelling is active, especially in the eastern Pacific. At about 140°W no cold upwelled water appears at the surface. F12 undersaturations (from 95°W to 130°W) correspond to an average upwelling velocity of $0.5 \pm 0.1 \text{ m d}^{-1}$, which is weak compared with other studies [*Wyrki*, 1981 ; *Halpern et al.*, 1989]. From this velocity, a new production caused by local upwelling is estimated as $11.4 \pm 1.8 \text{ mmolC m}^{-2} \text{ d}^{-1}$. We should however comment that the January-March 1991 upwelling was weaker than that of a few months earlier [NOAA 1991].

Because of the upwelling of cold thermocline water, the equatorial Pacific is supersaturated in PCO_2 with respect to the atmosphere and is a strong source of CO_2 for the atmosphere.

with an average flux of $4.88 \text{ mmolC m}^{-2} \text{ d}^{-1}$ for this cruise [Lefèvre and Dandonneau, 1992] compared to $1.23 \text{ mmolC m}^{-2} \text{ d}^{-1}$ for the equatorial Atlantic between 2.5°S and 2.5°N from Andrié *et al.* [1986]. The low chlorophyll concentrations we encountered show that production was probably limited by grazing or lack of iron at the time of the cruise. However the biological activity is the most important in causing the changes of PCO₂ in surface waters. The new production averages $72 \pm 25 \text{ mmolC m}^{-2} \text{ d}^{-1}$ ($0.9 \pm 0.3 \text{ gC m}^{-2} \text{ d}^{-1}$), i.e., one order of magnitude greater than the CO₂ evasion flux. This estimate is higher than all the previous estimates by other authors and is possibly the effect of our simplistic approach. The relative influence of biology, thermodynamics and outgassing on PCO₂ is however valid. Daily thermodynamical and biological variations of CO₂ show a great variability and no east-west trend appears (from 130°W to 165°E).

As was noted earlier, one of the major limitations of this study is the lack of adequate information on the circulation. This should be partially corrected in the future because of a comprehensive effort to sample the equatorial Pacific surface by drifter that has taken place since 1989. The data set represents a snapshot of the properties of the equatorial Pacific and more than one survey would be necessary to constrain the global carbon cycle. We are also hopeful that the improvements of the numerical models and wind forcings will make it possible to realistically simulate the circulation during the time of the ALIZE 2 cruise and to test the relative importance of the various processes controlling PCO₂.

Appendix: Zonal and Meridional Sections of Surface Properties

Distribution at the Equator

The equatorial distributions of surface nitrate, phosphate, silicate, temperature, salinity, PCO₂, F12, and chlorophyll *a* are given in figure A1. Temperature regularly increases to the west, and salinity is quite uniform in the western Pacific except for a decrease at 170°E . Upwelling produces the highest surface values of nutrients around 95°W . Nitrates decrease to the west as a result of the upwelling decrease noticeable in F12 distributions. Highest F12 undersaturations occur near 95°W , then the water becomes less undersaturated westward. The zonal gradients of nitrates in the central western Pacific exhibit fewer fluctuations than in the eastern Pacific where the currents were more variable. In particular, large meridional oscillations are present.

At 105°W , low values of nutrients are associated with warm ($T_{\text{max}} = 25.4^{\circ}\text{C}$) and fresher water ($S = 34$). At this longitude the distribution of F12 indicates near-equilibrium conditions and PCO₂ is relatively low (PCO₂ = $370 \mu\text{atm}$ and -0.5% saturation in F12), the mean atmospheric PCO₂ value was $349 \pm 5 \mu\text{atm}$ during the cruise. This water mass probably originates from the warm pool north of the equator and is drawn southward by the equatorial long waves [Eldin *et al.*, 1992].

Similar features, while less pronounced, are encountered at 128°W . The water is a little warmer and less dense and is

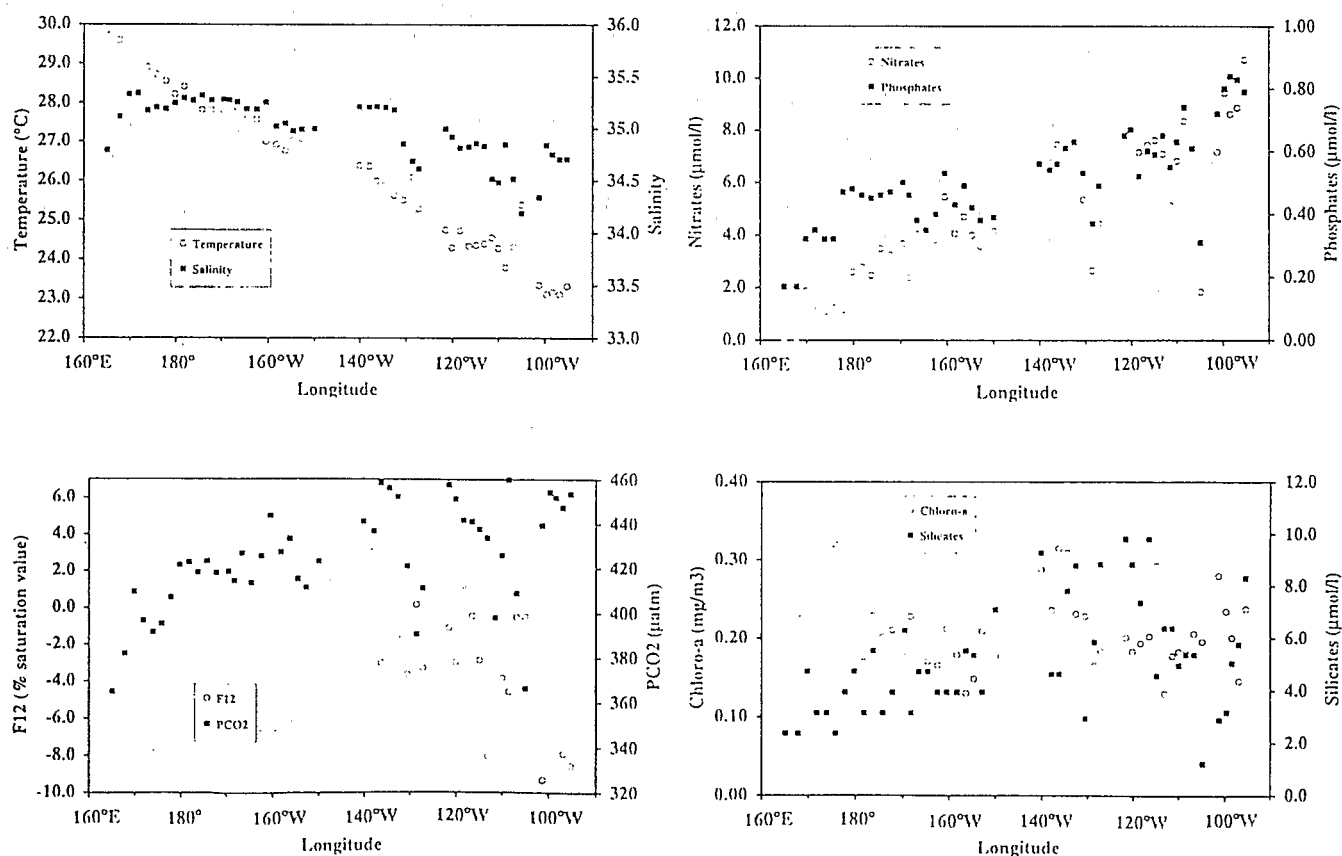


Figure A1. Surface properties versus longitude along the equator for SST, salinity, F12, PCO₂, nitrate, phosphate, chlorophyll *a*, and silicate.

characterized by lower nutrients and lower PCO_2 . Nevertheless, the atmospheric equilibrium conditions are not yet reached because this water is still slightly undersaturated in F12 and supersaturated in PCO_2 (390 μatm). These observations are similar to those encountered in the northern part of the transects at 110°W and 140°W . The equatorial Pacific is always supersaturated in PCO_2 except sometimes in the eastern Pacific where equatorial long waves are associated with important troughs in nutrient distributions and low PCO_2 . The westward decrease of PCO_2 due to CO_2 evasion and biological pump is counterbalanced by the warming which increases PCO_2 , and the oceanic PCO_2 remains above the atmospheric PCO_2 value.

95°W

The hydrological features associated with the equatorial upwelling are quite noticeable (Figure A2) in salinity and sea surface temperature with progressive warming and freshening

north of 1°N . At 1°N the surface temperature is 23.03°C and the salinity is 34.5, shifting to equal 25.8°C and 33.4 at 2°N , respectively. As F12 is a conservative tracer, its distribution contributes to the separation of the circulation from the biology. The most important F12 undersaturations are near 0° - 1°N (relative saturations $<91\%$) and are well correlated with nutrient distributions. The upwelled water is characterized by a temperature of 23°C , a mean salinity of 34.7 and high surface values of nitrates, phosphates, and silicates. It is likely that south of the equator the remnant of cold and salty waters must be more the result of meridional advection of upwelled waters than of upwelling itself, as the water is near the equilibrium conditions in F12. The largest surface supersaturations in PCO_2 extend from 1°S to 1°N . The surface maximum is located slightly north of the equator at 0.5°N and is consistent with the SST minimum of 22.8°C at 0.5°N .

The influence of the upwelling is not noticeable in silicates where low values appear at the surface south of the equator.

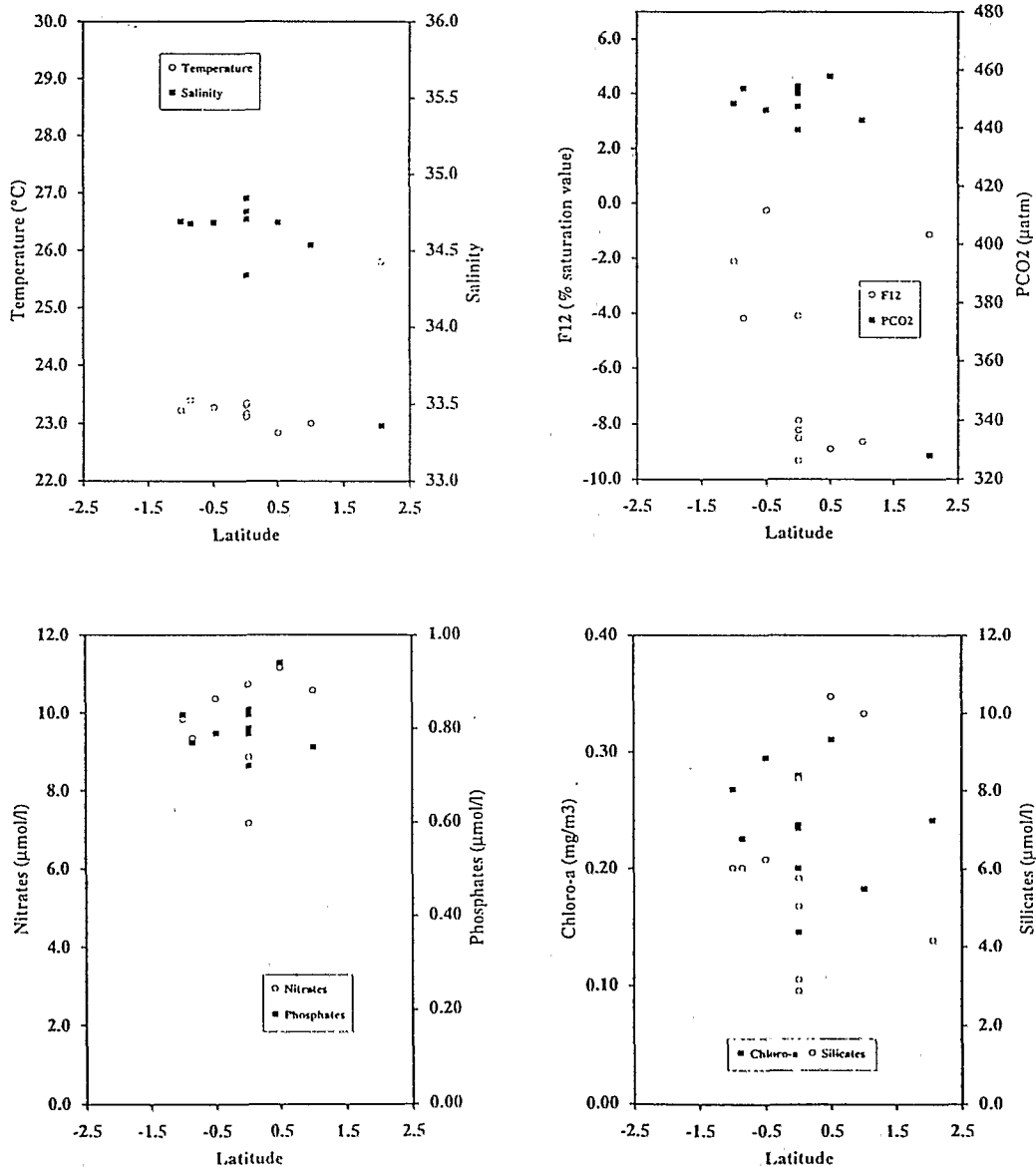


Figure A2. Surface properties versus latitude along 95°W for SST, salinity, F12, PCO_2 , nitrate, phosphate, chlorophyll *a*, and silicate.

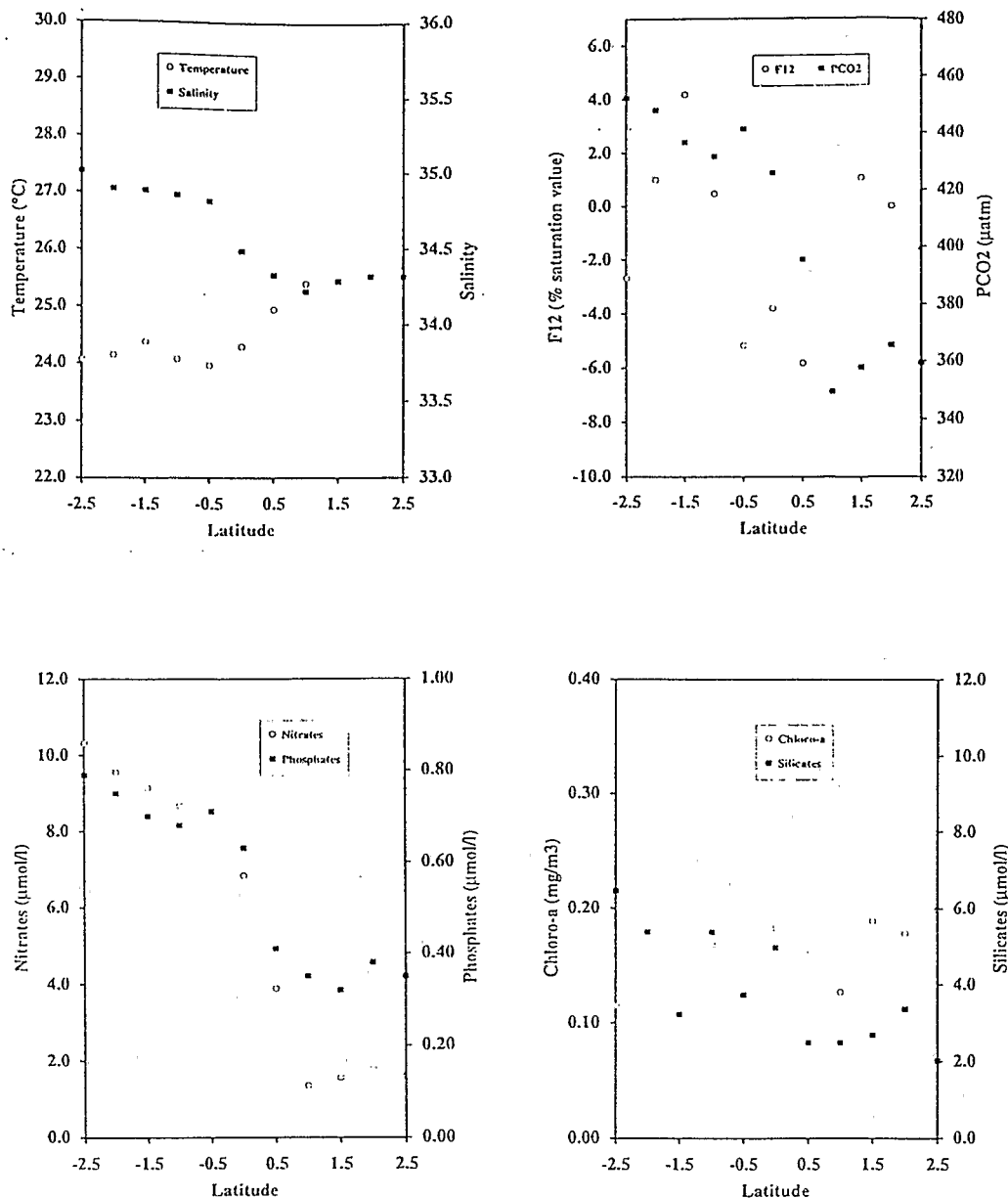


Figure A3. Surface properties versus latitude along 110°W for SST, salinity, F12, PCO₂, nitrate, phosphate, chlorophyll *a*, and silicate.

This depletion is probably caused by consumption by diatoms. North of 0.5°N, nutrients decrease and lower values are observed farther north. A peak of 0.31 mg m⁻³ in chlorophyll *a* is present; the decrease of chlorophyll starts after 0.5°S, while high values of nitrates and phosphates are present further south. The decrease in silicates is strong, suggesting that the bloom includes diatoms. Values of chlorophyll *a* are low in the equatorial Pacific but relatively high values are found in the upwelling zone (0.3 mg m⁻³) compared with values obtained during the cruise, confirming a biological activity. There is a north-south gradient in chlorophyll *a* which also seems to be also in nitrate distributions. In the absence of adequate measurements it is reasonable to generalize that the waters at 1.5°N-2°N, which are nearly equilibrated with the atmosphere, are low in nutrients as is also observed at other stations during the

cruise. Toward the west, at the equator, the water F12 is closer to saturation. High values of PCO₂ are maintained because the exchange with the atmosphere is slower and the warming increases PCO₂. The salinity increases, and the nutrients decrease while the chlorophyll increases.

Clearly, the water at 2°N is different from the upwelled water; it is warmer (25.8°C) and less dense (S=33.4), and the distribution of F12 shows that this water is close to equilibrium with the atmosphere. This water is undersaturated in PCO₂ and is a sink of CO₂ for the atmosphere.

110°W

The upwelling is weaker at 110°W (Figure A3) than at 95°W, according to the lower nutrient levels and smaller deviations from saturation equilibrium for CO₂ and F12 found in the sur-

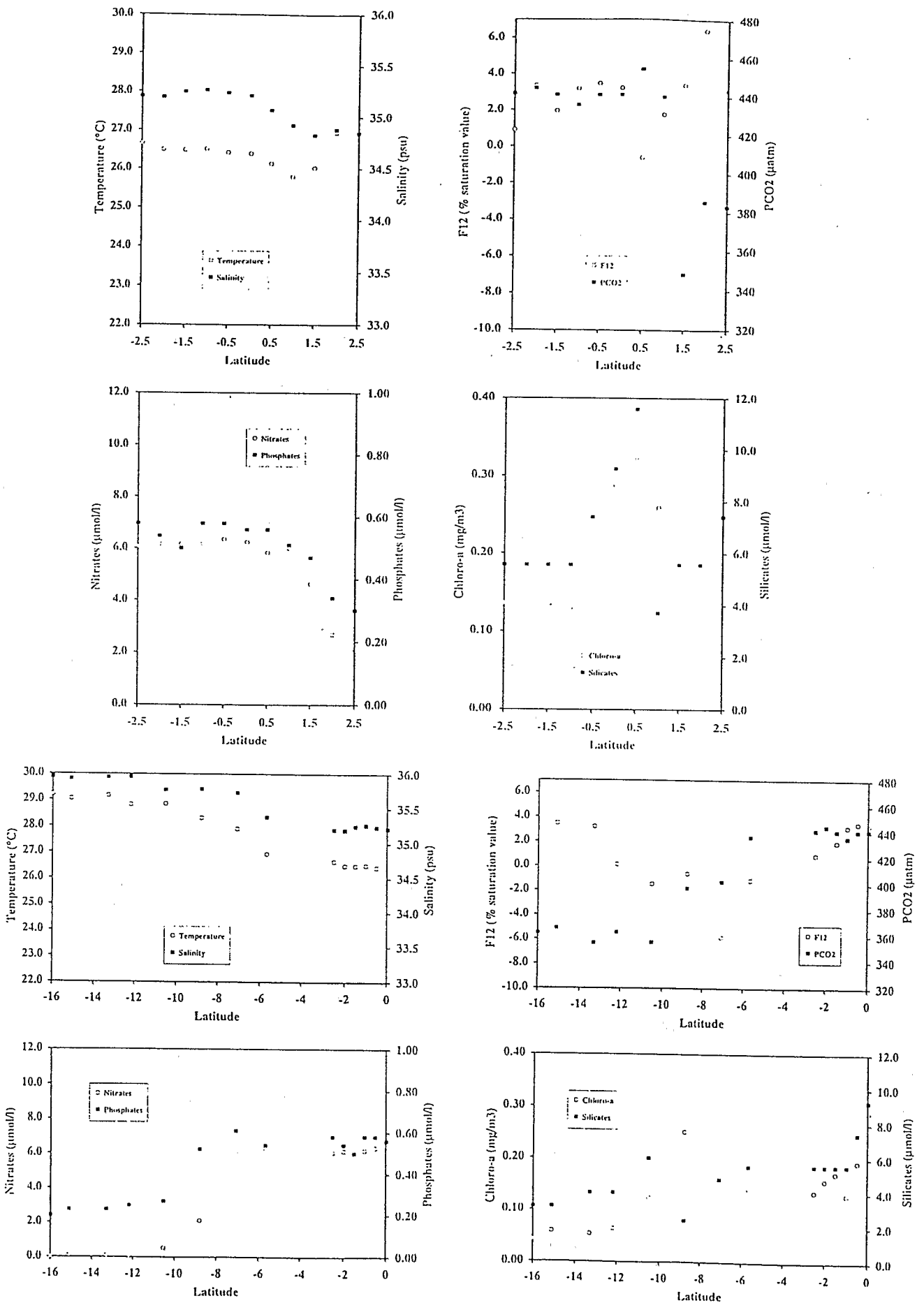


Figure A4. Surface properties versus latitude along (top) 140°W and 140°W-149°W (bottom) for SST, salinity, F12, PCO₂, nitrate, phosphate, chlorophyll *a*, and silicate.

face waters at 110°W. The distributions along the 110°W transect show a strong north-south asymmetry in temperature, salinity, NO₃, PO₄, F12, and PCO₂ distributions. The gradient is less pronounced on the silicate distribution. From 0.5°S to 1°N the water is undersaturated in F12, indicating that the upwelling occurs in this area. The maxima of PCO₂ and nutrients are observed south of the equator (2°S) suggesting an advection to the south of the upwelled water (SE current). The near equilibrium conditions in F12 show that the upwelling has not been recently active despite the high levels of nutrients, probably because nutrients are not consumed as fast as F12 reequilibrates with the atmosphere. The north-south asymmetry of nutrients (except for the silicates) is not found in the chlorophyll distribution. The distribution of chlorophyll *a* is quite uniform and low. High nutrient-low chlorophyll waters (HNLC) are observed in the south.

At 1°N, SST, salinity, PCO₂, and NO₃ distributions suggest that upwelling is not active. From 1.5°N to 2.5°N the water is near the equilibrium conditions and is even slightly supersaturated in F12 because of the warming effect. The absence of up-

welling north of 1.5°N is associated with low CO₂ and nutrient concentrations that correspond to the intrusion of warm and less dense water from the northwest. In the north, surface waters are warmer (25°C) and display a low salinity (34.2) comparable to the that found at the equator at 105°W.

140°W-149°W

At 140°W, to the north the water is supersaturated in F12 (Figure A4), which can originate from the warming effect on an initially undersaturated upwelled water. Because of rapid exchange (10-100 days) and warmer upwelled water the F12 is still near the equilibrium with the atmosphere even near the equator. The meridional temperature transect indicates that the upwelling is centered at 1°N. Near the equator the westward surface current is divided into two parts by a current flowing toward the northeast. The southwestward current (south of 1°N) is associated with high values of nitrates.

At 5.5°S, temperature and salinity increase and nitrates and PCO₂ decrease. A large change in the currents is present at 7.5°S. This change is also identified in the temperature and

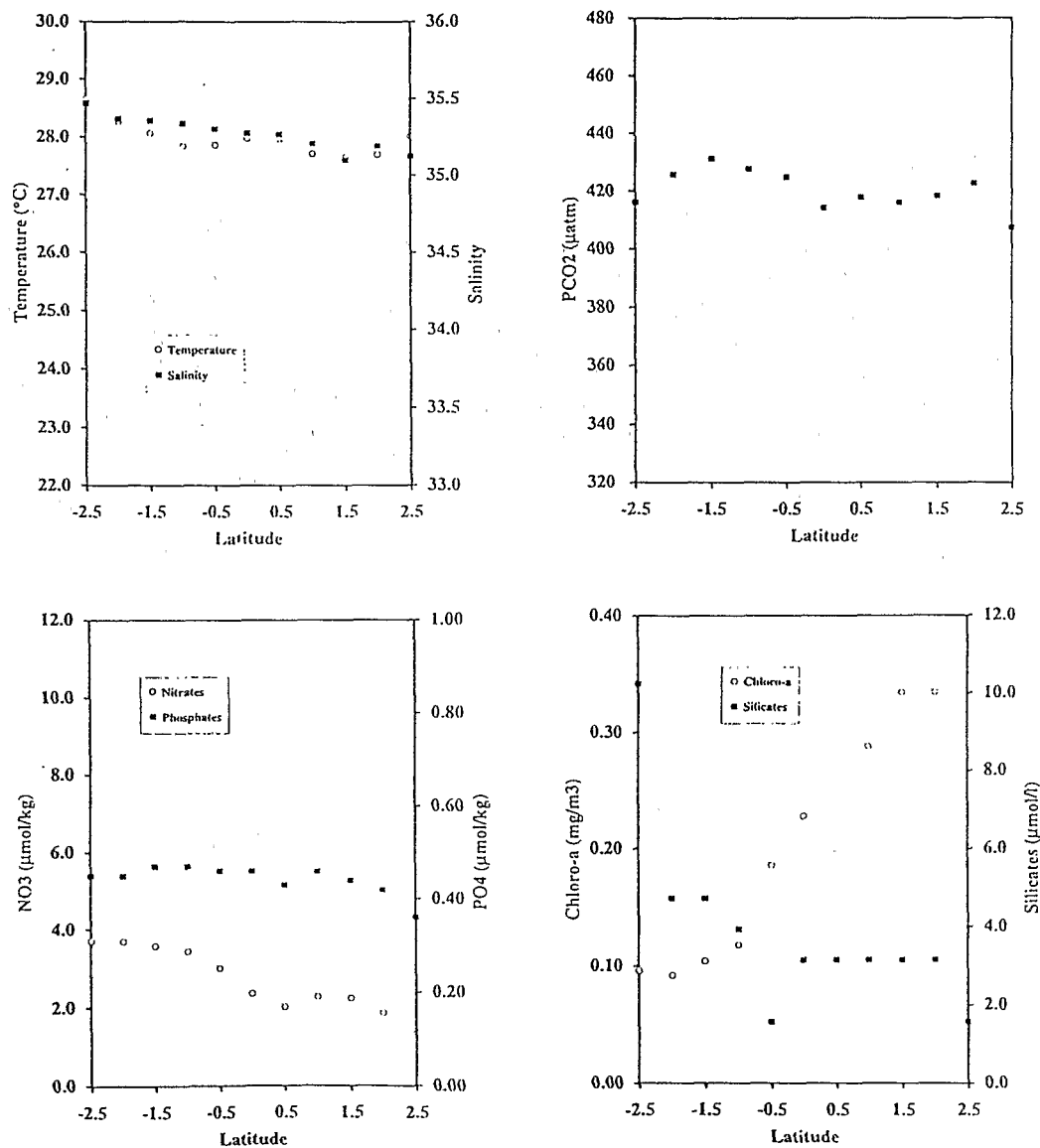


Figure A5. Surface properties versus latitude along 168°W for SST, salinity, F12, PCO₂, nitrate, phosphate, chlorophyll *a*, and silicate.

salinity plots and this latitude is associated with an undersaturation in F12. The southwestward current reverses and becomes southeastward and weak at the latitude of the Marquises islands. South of this latitude, temperature and salinity increase owing to the intense evaporation south of 13°S [Hayes, 1986; Rancher et Rougerie, 1992]. The nitrate and silicate decrease is correlated with a chlorophyll increase. Where nitrates are depleted, chlorophyll concentrations are less, so that nitrates seem to be a limiting factor for the development of phytoplankton south of this area.

168°W

The meridional distribution of surface temperature and salinity is quite uniform (Figure A5) and the upwelling does not appear clearly. No surface supply of nutrients is visible. Nitrates are lower north of the equator where chlorophyll is relatively high (0.33 mg m⁻³), suggesting that these low values in nutrients probably result from the consumption by phytoplankton. The decrease of chlorophyll is associated with a

strong northwestward current. Nutrients values are very similar to those found by Feely et al. [1987] on the 170°W transect (April 1984) except that they observed the upwelling clearly centered at the equator whereas we reported high and constant temperatures here. Wong et al. [1993] reported lower temperatures between 170°W-180°W during non El-Niño periods. They observed the typical peak of nutrients within the equator between 170°W-180°W during non El-Niño periods. The absence of this peak during the cruise ALIZE 2 confirms the weakness of the upwelling. The high uniform values of PCO₂ are probably the result of advection and warming as well as of the relatively long response time (3-6 months) for CO₂ to reach equilibrium with the atmosphere.

165°E

The distribution of surface temperature and salinity (Figure A6) is very similar to that of 168°W. The temperatures are the highest observed along the cruise and the salinity is low. The water is very poor in phosphate and completely depleted in ni-

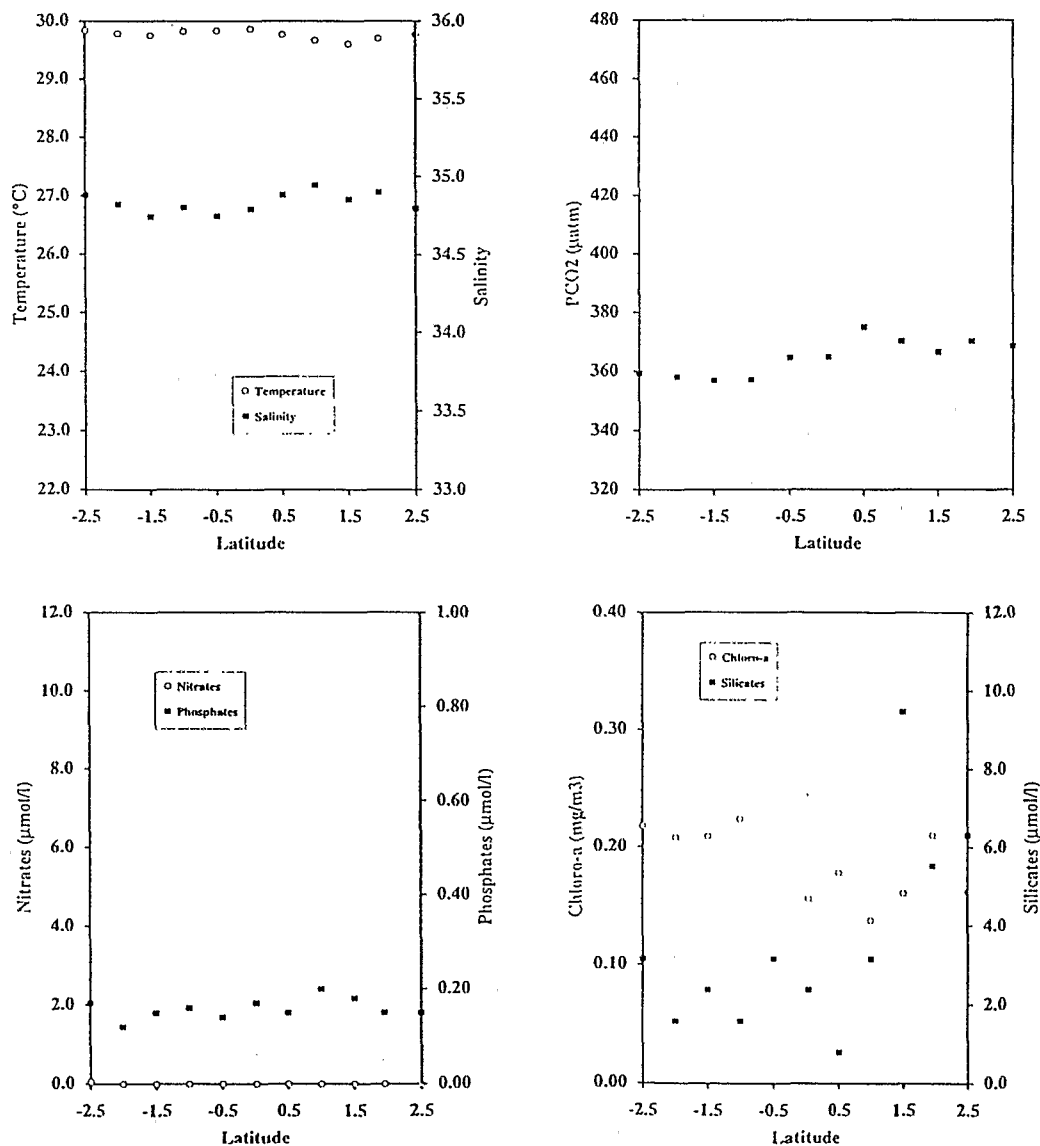


Figure A6. Surface properties versus latitude along 165°E for SST, salinity, F12, PCO₂, nitrate, phosphate, chlorophyll *a*, and silicate.

trate. The limiting factor for biological production seems to be nitrate. The distribution of chlorophyll is low and uniform. Surface waters are slightly supersaturated in CO₂: No influence from upwelling is noticeable, and warming effects and weak biological activity seem to be present in this region.

Acknowledgments. This work was supported by ORSTOM/CNRS (TOGA, PNEDC). We are very grateful to Philippe Gérard for nutrient analysis on board and Jean-Louis Crémoux and Jacques Grelet for their technical help. We also wish to thank Aubert Le Bouteiller and Jean Blanchot for their comments and helpful suggestions and Gérard Eldin for providing ADCP currents. We finally thank all the crew of the N/O Noroit (IFREMER).

References

- Andrié, C., C. Oudot, C. Genthon, and L. Merlivat, CO₂ fluxes in the tropical Atlantic during FOCAL cruises, *J. Geophys. Res.*, **91**, 11,741-11,755, 1986.
- Broecker, W.S., J.R. Ledwell, T. Takahashi, R. Weiss, L. Merlivat, L. Memery, T.H. Peng, N. Jähne, and K.O. Munnich, Isotopic versus micrometeorologic ocean CO₂ fluxes: A serious conflict, *J. Geophys. Res.*, **91**, 10,517-10,527, 1986.
- Bullister, J.L., and R.F. Weiss, Determination of CCl₃F and CCl₂F₂ in seawater and air, *Deep Sea Res.*, **35**, 839-853, 1988.
- Chavez, F.P., and R.T. Barber, An estimate of new production in the equatorial Pacific, *Deep Sea Res.*, **34**, 1229-1243, 1987.
- Copin-Montégut, C., A new formula for the effect of temperature on the partial pressure of CO₂ in seawater, *Mar. Chem.*, **25**, 29-37, 1988.
- Copin-Montégut, C., A new formula for the effect of temperature on the partial pressure of CO₂ in seawater, *Cortigendum, Mar. Chem.*, **27**, 143-144, 1989.
- Cullen, J.J., M.R. Lewis, C.O. Davis, and R.T. Barber, Photosynthetic characteristics and estimated growth rates indicate grazing is the proximate control of primary production in the equatorial Pacific, *J. Geophys. Res.*, **97**, 639-654, 1992.
- Dugdale, R.C., F.P. Wilkerson, R.T. Barber, and F.P. Chavez, Estimating new production in the equatorial Pacific ocean at 150°W, *J. Geophys. Res.*, **97**, 681-686, 1992.
- Eldin, G., A. Morlière, and G. Reverdin, Acoustic doppler current profiling along the Pacific equator from 95°W to 165°E, *Geophys. Res. Lett.*, **19**, 913-916, 1992.
- Feely, R.A., R.H. Gammon, B.A. Taft, P.E. Pullen, L.S. Waterman, T.J. Conway, J.F. Gendron, and D.P. Wisegaver, Distribution of chemical tracers in the eastern Equatorial Pacific during and after the 1982-1983 El Niño/Southern Oscillation event, *J. Geophys. Res.*, **92**, 6545-6558, 1987.
- Fiedler, P.C., F.P. Chavez, D.W. Behringer, and S.B. Reilly, Physical and biological effects of Los Niños in the eastern tropical Pacific, 1986-1989, *Deep Sea Res.*, **39**, 199-219, 1992.
- Garçon, V., F. Thomas, C.S. Wong, and J.F. Minster, Gaining insight into the seasonal variability of CO₂ at ocean station P using an upper ocean model, *Deep Sea Res.*, **39**, 921-938, 1992.
- Halpern, D., Vertical motion at the equator in the eastern Pacific (abstract), *Eos, Trans. AGU*, **61**, 998, 1980.
- Halpern, D., R.A. Knox, E.S. Luther, and S.G.H. Philander, Estimate of equatorial upwelling between 140° and 110°W during 1984, *J. Geophys. Res.*, **94**, 8018-8020, 1989.
- Hayes, S.P., The circulation of the equatorial Pacific ocean, paper presented at the U.S. Tropical Ocean and Global Atmosphere Workshop on the Dynamics of the Equatorial Oceans, Nova University Press, Florida, Honolulu, Hawaii, August 11-15, 1986.
- Inoue, H.Y., and Y. Sugimura, Variations and distributions of CO₂ in and over the equatorial Pacific during the period from the 1986/88 El Niño event to the 1988/89 La Niña event, *Tellus, 44B*, 1-22, 1992.
- Le Bouteiller, A., and J. Blanchot, Size distribution and abundance of phytoplankton in the Pacific equatorial upwelling, *La mer*, **29**, 175-179, 1991.
- Le Bouteiller, A., J. Blanchot, and M. Rodier, Size distribution of phytoplankton in the western Pacific: Towards a generalization for the tropical open ocean, *Deep Sea Res.*, **39**, 805-823, 1992.
- Lefèvre, N., and Y. Daulonnet, CO₂ fluxes in the equatorial Pacific during January-March 1991, *Geophys. Res. Lett.*, **22**, 2223-2226, 1992.
- Liss, P.S., and L. Merlivat, Air-sea gas exchange rates: Introduction and synthesis, in *The Role of Air-Sea Exchange in Geochemical Cycling*, edited by P. Buat-Ménard, *NATO/ASI Ser., C185*, 113-127, 1986.
- Minas, H.J., and M. Minas, Net community production in High Nutrient-Low Chlorophyll waters of the tropical and Antarctic oceans: Grazing vs iron hypothesis, *Oceanol. Acta*, **15**, 145-162, 1992.
- Murphy, P.P., R.A. Feely, R.H. Gammon, D.E. Harrison, K.C. Kelly, and L.S. Waterman, Assessment of the air-sea exchange of CO₂ in the south Pacific during austral autumn, *J. Geophys. Res.*, **96**, 20,455-20,465, 1991.
- National Oceanic and Atmospheric Administration (NOAA), Climate Diagnostics Bulletin, *rep. 90/11-90/12*, Climate Analysis Center, Washington, D.C., 1990.
- National Oceanic and Atmospheric Administration (NOAA), Climate Diagnostics Bulletin, *rep. 91/1-91/2*, Climate Analysis Center, Washington, D.C., 1991.
- Oudot, C., and C. Andrié, Short-term changes in the partial pressure of CO₂ in eastern tropical Atlantic surface seawater and in atmospheric CO₂ mole fraction, *Tellus, 41B*, 537-553, 1989.
- Oudot, C., and Y. Montel, A high sensitivity method for the determination of nanomolar concentrations of nitrate and nitrite in seawater with a Technicon Autoanalyser II, *Mar. Chem.*, **24**, 239-252, 1988.
- Poulain, P.M., Estimates of horizontal divergence and vertical velocity in the equatorial Pacific, *J. Phys. Oceanogr.*, **23**, 601-607, 1993.
- Rancher, J., and F. Rougerie, Situations océaniques du Pacifique central sud, campagnes du B.O.C.B. "Marara" d'avril 1986 à octobre 1989, *HYDROPOL*, edited by Service Mixte de Sécurité Radiologique, 86 pp., Monthéry, France, 1992.
- Reverdin, G., A. Morlière, and G. Eldin, ALIZE II, campagne océanographique trans-Pacifique, recueil de données, *Int. Rep.*, **91-13**, 341 pp., Lab. Oceanogr. Dyn. et de Climatol., Univ. de Paris, CNRS, 1991.
- Robertson, J.E., A.J. Watson, C. Langdon, R.D. Ling and J.W. Wood, Diurnal variation in surface pCO₂ and O₂ at 60°N, 20°W in the North Atlantic, *Deep Sea Res.*, **40**, 409-422, 1993.
- Smethie, W.M., T. Takahashi, D.W. Chipman, and J.R. Ledwell, Gas exchange and CO₂ flux in the tropical Atlantic ocean determined from radon and PCO₂ measurements, *J. Geophys. Res.*, **90**, 7005-7022, 1985.
- Strickland, J., and T. Parsons, A practical handbook of seawater analysis, *Bull. Fish. Res. Board Can. Bull.*, **167**, 310 pp., 1972.
- Thomas, F., V. Garçon, and J.F. Minster, Modelling the seasonal cycle of dissolved oxygen in the upper ocean at Ocean Weather Station P, *Deep Sea Res.*, **37**, 463-491, 1990.
- Walsh, J.J., Herbivory as a factor in patterns of nutrient utilization in the sea, *Limnol. and Oceanogr.*, **21**, 1-13, 1976.
- Warner, M.J., Chlorofluoromethanes F11 and F12: Their solubilities in water and seawater and studies of their distributions in the South Atlantic and North Pacific oceans, Ph. D. dissertation, 124 pp., Univ. of Calif., San Diego, 1988.
- Warner, M.J., and R.F. Weiss, Solubilities of chlorofluorocarbons 11 and 12 in water and seawater, *Deep Sea Res.*, **32**, 1485-1497, 1985.
- Watson, A.J., C. Robinson, J.E. Robinson, P.J.B. Williams, and M.J.R. Fasham, Spatial variability in the sink for atmospheric carbon dioxide in the North Atlantic, *Nature*, **350**, 50-53, 1991.
- Weare, B.C., P.T. Strub, and M.D. Samuel, Annual mean surface heat

- fluxes in the tropical Pacific ocean. *J. Phys. Oceanogr.*, *11*, 705-717, 1981.
- Weiss, R.F., R.A. Jahnke, and C.D. Keeling. Seasonal effects of temperature and salinity on the partial pressure of CO₂ in seawater. *Nature*, *300*, 511-513, 1982.
- Wong, C.S. and Y.H. Chan. Temporal variations in the partial pressure and flux of CO₂ at ocean station P in the subarctic northeast Pacific ocean. *Tellus*, *43B*, 206-223, 1991.
- Wong, C.S., Y.H. Chan, J.S. Page, G.E. Smith, and R.D. Bellegay. Changes in equatorial CO₂ flux and new production estimated from CO₂ and nutrient levels in Pacific surface waters during the 1986/87 El Niño. *Tellus*, *45B*, 64-79, 1993.
- Wyrski, K., An estimate of equatorial upwelling in the Pacific. *J. Phys. Oceanogr.*, *11*, 1205-1214, 1981.
- C. Andrié, Y. Dandonneau, and N. Lefèvre. Laboratoire d'Océanographie Dynamique et de Climatologie, University of Paris VI, T. 24, 2^{ème} étage, 75252 Paris Cedex 05, France. (e-mail: andrie@lodyc.jussieu.fr; yd@lodyc.jussieu.fr; nl@lodyc.jussieu.fr)
- G. Reverdin, Lamont-Doherty Earth Observatory, Palisades, NY 10964. (e-mail: reve@rainbow.ligo.columbia.edu)
- M. Rodier, Institut Français de Recherche Scientifique pour le Développement en Coopération, BP A5, Nouméa, New Caledonia. (e-mail: rodier@orstom.orstom.fr)

(Received May 17, 1993; revised January 25, 1994; accepted February 2, 1994.)